

Theoretical Methods Enlighten Magnetic Properties of a Family of Mn₆ Single-Molecule Magnets

Eduard Cremades,[†] Joan Cano,^{†,‡} Eliseo Ruiz,^{*,†} Gopalan Rajaraman,^{*,§} Constantinos J. Milios,^{||,⊥} and Euan K. Brechin^{*,⊥}

[†]Departament de Química Inorgànica and Institut de Recerca de Química Teòrica i Computacional, Universitat de Barcelona, Diagonal 647, 08028 Spain, [‡]Institució Catalana de Recerca i Estudis Avançats (ICREA), Passeig Lluís Companys 23, 08010 Barcelona, Spain, [§]Dipartimento di Chimica, Università di Firenze, Polo Scientifico di Sesto Fiorentino, 50019 Sesto Fiorentino, Italy, ^{||}Department of Chemistry, University of Crete, 71003 Herakleion, Greece, and [⊥]School of Chemistry, The University of Edinburgh, West Mains Road, Edinburgh EH9 3JJ, United Kingdom

Received May 20, 2009

Magnetic properties of the family of Mn₆ complexes with oximate bridging ligands, some of them showing the highest anisotropy energy barriers known to date, have been studied using theoretical methods based on density functional theory. The different magnetic behaviors, total spin values from 4 to 12, are well reproduced by the calculated exchange coupling constants. The analysis of the magnetostructural correlations indicates that the Mn–N–O–Mn torsion angles play a crucial role, with the out-of-plane shift of the central oxo bridging ligand involved to a lesser degree. The Mn–N–O–Mn torsion angles are mainly controlled by the existence of an intramolecular hydrogen bond between the NO group of the bridging ligand and the substituents of the equatorial oximate bridging ligand and the presence of bulky substituents in the axial carboxylate ligands.

Introduction

Since the discovery in 1993 of single-molecule magnet (SMM) behavior by Gatteschi and co-workers in a Mn₁₂ compound,^{1,2} one single molecule of this compound behaves like a magnet, many research groups have intensively searched for new molecules showing such appealing properties.³ Slow relaxation of the magnetization at low temperature is responsible for the presence of a hysteresis loop in magnetization curves, which also display some irregular shapes because of the presence of thermally induced quantum tunneling.^{4,5} To have slow relaxation of the magnetization, the states with positive and negative magnetic moments must be separated by an energy barrier, whose height is known to depend directly on the square of the total spin of the molecule and on its magnetic anisotropy. Such transition metal complexes are much sought after synthetic targets because of their potential as systems that could eventually lead to applications for information storage

at the molecular level if the barrier is high enough to avoid the thermal jump or the quantum tunneling effects. Despite the fact that many single-molecule magnets have been synthesized during the last fifteen years only recently have some of them shown a higher barrier than the originally studied Mn₁₂ complex.³ This goal was achieved with a new family of Mn₆ complexes with oximate and oxo bridging ligands that were synthesized by Milios et al. displaying a variety of total spin and magnetic anisotropy values (Table 1).^{6–11} The total spin values range from $S = 4$ for complex **1**^{12,13} (see Figure 1) to **12**,

*To whom correspondence should be addressed. E-mail: eliseo.ruiz@qi.ub.es.

(1) Caneschi, A.; Gatteschi, D.; Sessoli, R.; Barra, A. L.; Brunel, L. C.; Guillot, M. *J. Am. Chem. Soc.* **1991**, *113*, 5873.

(2) Sessoli, R.; Gatteschi, D.; Caneschi, A.; Novak, M. A. *Nature* **1993**, *365*, 141.

(3) Aromí, G.; Brechin, E. *Struct. Bonding (Berlin, Ger.)* **2006**, *122*, 1.

(4) Gatteschi, D.; Sessoli, R. *Angew. Chem., Int. Ed.* **2003**, *42*, 246.

(5) Gatteschi, D.; Sessoli, R.; Villain, J. *Molecular Nanomagnets*; Oxford University Press: Oxford, 2006.

(6) Milios, C. J.; Vinslava, A.; Wood, P. A.; Parsons, S.; Wernsdorfer, W.; Christou, G.; Perlepes, S. P.; Brechin, E. K. *J. Am. Chem. Soc.* **2007**, *129*, 8.

(7) Milios, C. J.; Vinslava, A.; Wernsdorfer, W.; Prescimone, A.; Wood, P. A.; Parsons, S.; Perlepes, S. P.; Christou, G.; Brechin, E. K. *J. Am. Chem. Soc.* **2007**, *129*, 6547.

(8) Milios, C. J.; Inglis, R.; Vinslava, A.; Bagai, R.; Wernsdorfer, W.; Parsons, S.; Perlepes, S. P.; Christou, G.; Brechin, E. K. *J. Am. Chem. Soc.* **2007**, *129*, 12505.

(9) Milios, C. J.; Piligkos, S.; Brechin, E. K. *Dalton Trans.* **2008**, 1809.

(10) Milios, C. J.; Inglis, R.; Bagai, R.; Wernsdorfer, W.; Collins, A.; Moggach, S.; Parsons, S.; Perlepes, S. P.; Christou, G.; Brechin, E. K. *Chem. Commun.* **2007**, 3476.

(11) Jones, L. F.; Cochrane, M. E.; Koivisto, B. D.; Leigh, D. A.; Perlepes, S. P.; Wernsdorfer, W.; Brechin, E. K. *Inorg. Chim. Acta* **2008**, *361*, 3420.

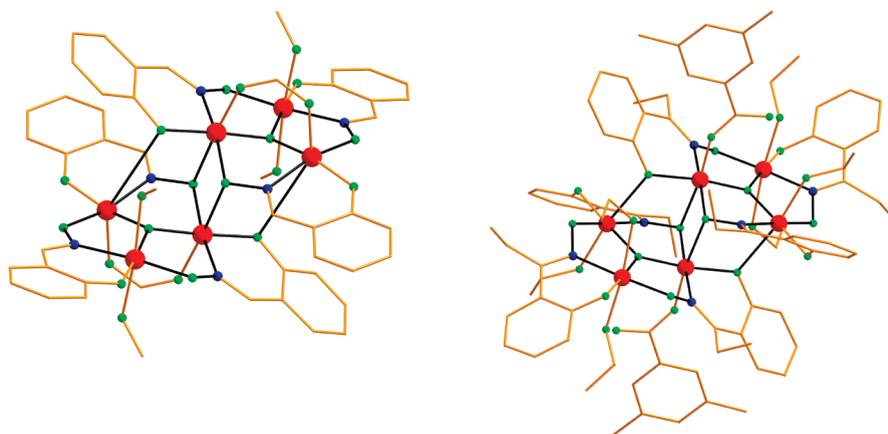
(12) Milios, C. J.; Manoli, M.; Rajaraman, G.; Mishra, A.; Budd, L. E.; White, F.; Parsons, S.; Wernsdorfer, W.; Christou, G.; Brechin, E. K. *Inorg. Chem.* **2006**, *45*, 6782.

(13) Milios, C.; Raptopoulou, C. P.; Terzis, A.; Lloret, F.; Vicente, R.; Perlepes, S.; Escuer, A. *Angew. Chem., Int. Ed.* **2004**, *43*, 210.

Table 1. Experimental Data Corresponding to the Family of the Mn₆ Complexes (1–12,⁸ 13–15,¹¹ 16¹³), the Values of the Mn–N–O–Mn Torsion Angles and out-of-Plane Shift (*h*) of the Central Oxygen Atom and the Magnetic Data, Fitted Exchange Coupling Constants, Total Spin of the Ground State, and Energy Barrier (*U*_{eff}) Due to the Anisotropy of the Molecule

complex	Mn–N–O–Mn (deg)	<i>h</i> (Å)	<i>J</i> (cm ⁻¹)	<i>S</i>	<i>U</i> _{eff} (K)
[Mn ₆ O ₂ (H-sao) ₆ (O ₂ CH) ₂ (MeOH) ₄] (1)	18.0, 10.4, 25.6	-0.228 ^a	-4.6, -1.8, +1.25	4	28
[Mn ₆ O ₂ (Me-sao) ₆ (O ₂ CCPh ₃) ₂ (EtOH) ₄] (2)	42.4, 25.5, 29.7	0.076	+1.2, -1.95	4	31.7
[Mn ₆ O ₂ (Et-sao) ₆ (O ₂ CCMe ₃) ₂ (EtOH) ₃] (3)	42.1, 36.9, 23.3	0.072	+1.39, -1.92	6	30
	42.2, 16.7, 32.4	0.107			
[Mn ₆ O ₂ (Et-sao) ₆ (O ₂ CPh ² OPh) ₂ (EtOH) ₄] (4)	47.6, 23.7, 31.8	0.061	+1.76, -1.92	7	43.2
[Mn ₆ O ₂ (Et-sao) ₆ (O ₂ CPh ⁴ OPh) ₂ (EtOH) ₄ (H ₂ O) ₂] (5)	43.7, 38.3, 30.3	0.059	+1.39, -0.99	9	56.9
[Mn ₆ O ₂ (Me-sao) ₆ (O ₂ CPhBr) ₂ (EtOH) ₆] (6)	42.9, 31.9, 30.4	0.085	+1.15, -0.73	11	50.2
[Mn ₆ O ₂ (Et-sao) ₆ (O ₂ CPh) ₂ (EtOH) ₄ (H ₂ O) ₂] (7)	39.9, 38.2, 31.3	0.092	+0.93	12	53.1
[Mn ₆ O ₂ (Et-sao) ₆ (O ₂ CPh(Me) ₂) ₂ (EtOH) ₆] (8)	43.1, 39.1, 34.9	0.039	+1.63	12	86.4
[Mn ₆ O ₂ (Et-sao) ₆ (O ₂ C ₁₁ H ₁₅) ₂ (EtOH) ₆] (9)	42.6, 36.7, 34.0	0.055	+1.60	12	79.9
[Mn ₆ O ₂ (Me-sao) ₆ (O ₂ C-th) ₂ (EtOH) ₄ (H ₂ O) ₂] (10)	31.1, 36.3, 27.4	0.033	n.a.	n.a.	n.a.
[Mn ₆ O ₂ (Et-sao) ₆ (O ₂ CPhMe) ₂ (EtOH) ₄ (H ₂ O) ₂] (11)	47.2, 38.2, 30.4	0.082	+1.85, -0.70	12	69.9
[Mn ₆ O ₂ (Et-sao) ₆ (O ₂ C ₁₂ H ₁₇) ₂ (EtOH) ₄ (H ₂ O) ₂] (12)	41.5, 40.1, 27.8	0.103	+1.55, -2.20	5 ± 1	31.2
[Mn ₆ O ₂ (Et-sao) ₆ (O ₂ CNaph) ₂ (EtOH) ₄ (H ₂ O) ₂] (13)	41.1, 33.3, 40.5	0.105	+1.31	12	60.1
[Mn ₆ O ₂ (Et-sao) ₆ (O ₂ CAnth) ₂ (EtOH) ₄ (H ₂ O) ₂] (14)	42.3, 39.3, 25.6	0.097	+1.75, -0.90	12	60.1
[Mn ₆ O ₂ (Et-sao) ₆ (O ₂ CPhCCH) ₂ (EtOH) ₄ (H ₂ O) ₂] (15)	38.9, 38.7, 32.1	0.076	+0.79	12	66.8
[Mn ₆ O ₂ (H-sao) ₆ (O ₂ CCH ₃) ₂ (EtOH) ₄] (16)	22.8, 16.5, 10.7	-0.215 ^a	-3.5, -12.6, +12.4, -0.45	4	28

^aNegative sign means inward shift.

**Figure 1.** Representation of the molecular structure of complexes 1 (left) and 8 (right) (see Table 1). Large red spheres are the Mn atoms, while oxygen and nitrogen atoms are represented by small green and blue spheres, respectively. The carbon atoms are represented as orange cylinders to simplify the figure.

the latter being with a total spin expected for a ferromagnetically coupled system with the energy barrier related to the magnetic anisotropy (complex 8, see Figure 1) higher than any other SMM.¹⁴ Recently, the effect of the pressure on the magnetic properties of these complexes has also been analyzed.¹⁵ An analysis of the structural parameters for such complexes was performed and two parameters were selected as those that could possibly control the magnetic properties, namely, the distortion of the Mn–N–O–Mn torsion angle and the out-of-plane shift of the bridging oxo ligand.

A full characterization of the exchange interactions should provide us with valuable information for the future design of new molecular systems with still improved magnetic

properties.¹⁶ However, from the experimental point of view the knowledge of the exchange interactions that determine the spin states of large polynuclear complexes are not easily obtained from the temperature dependence of the magnetic susceptibility because there are usually many parameters (many sets of them) that can reproduce the experimental data perfectly.¹⁷ During the past few years, some of us have extensively employed theoretical methods based on density functional theory (DFT) to obtain the exchange coupling constants of large polynuclear complexes with remarkable success taking into account the subtle energy differences involved in the magnetic properties.^{18–22} Also recently, some

(14) Milios, C. J.; Vinslava, A.; Wernsdorfer, W.; Moggach, S.; Parsons, S.; Perlepes, S. P.; Christou, G.; Brechin, E. K. *J. Am. Chem. Soc.* **2007**, *129*, 2754.

(15) Prescimone, A.; Milios, C. J.; Moggach, S.; Warren, J. E.; Lennie, A. R.; Sanchez-Benitez, J.; Kamenev, K.; Bircher, R.; Murrice, M.; Parsons, S.; Brechin, E. K. *Angew. Chem., Int. Ed.* **2008**, *47*, 2828.

(16) *Magnetism: Molecules to Materials*; Miller, J. S., Drillon, M., Eds.; Wiley-VCH: Weinheim, 2001–2005; Vols. 1–5.

(17) Ruiz, E. *Struct. Bonding (Berlin, Ger.)* **2004**, *113*, 71.

(18) Ruiz, E.; Alemany, P.; Alvarez, S.; Cano, J. *J. Am. Chem. Soc.* **1997**, *119*, 1297.

(19) Ruiz, E.; Alvarez, S.; Rodriguez-Fortea, A.; Alemany, P.; Pouillon, Y.; Massobrio, C. In *Magnetism: Molecules to Materials*; Miller, J. S., Drillon, M., Eds.; Wiley-VCH: Weinheim, 2001; Vol. 2, p 227.

(20) Ruiz, E.; Cano, J.; Alvarez, S. *Chem.—Eur. J.* **2005**, *11*, 4767.

(21) Ruiz, E.; Cauchy, T.; Cano, J.; Costa, R.; Tercero, J.; Alvarez, S. *J. Am. Chem. Soc.* **2008**, *130*, 7420.

(22) Ruiz, E.; Rodriguez-Fortea, A.; Cano, J.; Alvarez, S.; Alemany, P. *J. Comput. Chem.* **2003**, *24*, 982.

Table 2. Calculated Exchange Coupling Constants (J_1 – J_5 , see Figure 3) for the Six Studied Mn_6 Complexes Indicating the Experimental Mn–N–O–Mn Torsion Angles Corresponding to the J_1 – J_3 Interactions, and the Total Spin for the Ground and First Excited State^a

complex	Mn–N–O–Mn (deg)	J_{calc} (cm^{-1})	S_{calc}	S_{exc}
$[Mn_6O_2(H\text{-sao})_6(O_2CH)_2(MeOH)_4]$ (1)	18.0, 10.4, 25.6	–10.5, –3.1, +1.3 –0.5, +2.9	4	3 (9.0)
$[Mn_6O_2(Me\text{-sao})_6(O_2CCPh)_2(EtOH)_4]$ (2)	42.4, 25.5, 29.7	+1.2, –1.6, –1.5 –0.8, +3.2	4	3 (1.3)
$[Mn_6O_2(Et\text{-sao})_6(O_2CPh^+OPh)_2(EtOH)_4]$ (4)	47.6, 23.7, 31.8	+3.1, –3.4, +0.8 –0.2, +3.6	4	5 (4.3)
$[Mn_6O_2(Et\text{-sao})_6\{O_2CPh(Me)_2\}_2(EtOH)_6]$ (8)	43.1, 39.1, 34.9	+1.2, +2.6, +1.6 +0.5, +3.1	12	11 (5.3)
$[Mn_6O_2(Me\text{-sao})_6(O_2C\text{-th})_2(EtOH)_4(H_2O)_2]$ (10)	31.1, 36.3, 27.4	–2.3, +2.3, –1.8 –0.7, +2.1	4	3 (3.7)
$[Mn_6O_2(Et\text{-sao})_6(O_2C_{12}H_{17})_2(EtOH)_4(H_2O)_2]$ (12)	41.5, 40.1, 27.8	–0.02, +2.9, –0.9 +0.05, +3.3	4	3 (1.4)

^a The value in parentheses corresponds to the energy difference (in cm^{-1}) between such states.

of the authors of this paper performed theoretical analysis of the magnetostructural correlations of a family of Mn_3 complexes²³ that adopt structures with only one triangle of cations instead of the two present in the Mn_6 complexes,²⁴ although there are some differences between both families of complexes in terms of the different coordination of the bridging ligands (the presence of carboxylato bridging ligands). Some of us have also analyzed the relationship between the total spin and the magnetic anisotropy of the family of the Mn_6 complexes using density functional methods including spin–orbit effects.²⁵ The results show the predominance of the single-ion terms of the anisotropy, perhaps suggesting the energy barriers to be relatively independent of the total spin of the complex. Although, this is a matter of considerable current debate. Also, reaching similar conclusions Piligkos et al. have published a study analyzing the role of the ligand-field parameters in the magnetic anisotropy of the Mn_6 complexes.²⁶ Previously, some of us studied the magnetic properties of several $[Mn^{III}_2Mn^{II}_4]$ complexes possessing a similar structural motif to the present and have rationalized the difference in the observed magnetic properties using DFT calculations.²⁷

The goals of the present work are to study the magnetic properties of some of the Mn_6 complexes using theoretical methods based on DFT, to establish the sign and magnitude of the exchange coupling constants (J) within such systems, and to search for the structural factors that determine their magnetic properties. To that end we apply the computational tools that have successfully described the electronic and magnetic structures of a variety of polynuclear transition metal complexes using hybrid functionals and all electron basis sets.^{22,28,29}

Results and Discussion

Exchange Coupling Constants of the Mn_6 complexes. To carry out the theoretical study of the exchange coupling in

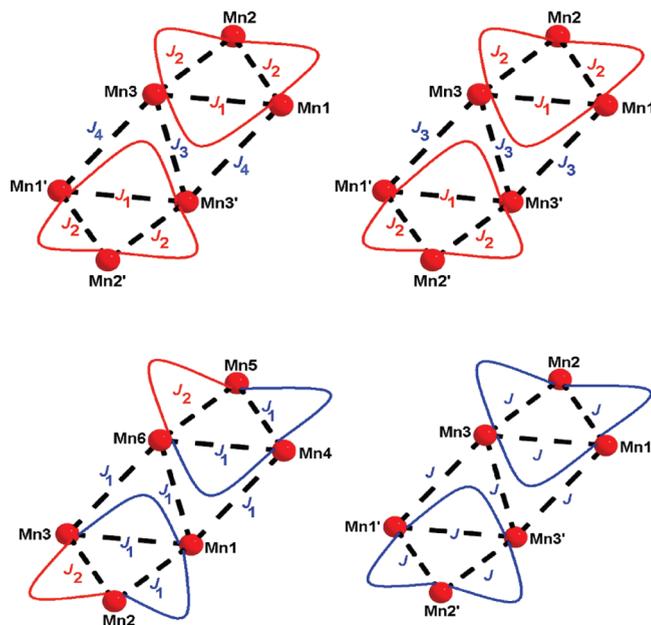


Figure 2. Description of the J value models (from 4 to 1 J values) employed to analyze the experimental magnetic susceptibility data depending of the number of fitted J values indicated in Table 1.

the family of Mn_6 complexes (see Table 2), we have selected six representative complexes (1, 2, 4, 8, 10, and 12), with the calculated J values collected in Table 2. From the experimental point of view (see Table 1) a smaller number of J constants (see Figure 2) were considered to avoid overparametrization, but this provides a somewhat unrealistic description of the system, giving average J values for the interactions.⁸ However, for the theoretical study we have considered all the exchange pathways to be different (J_1 – J_5 , see Figure 3) resulting in the following Heisenberg Hamiltonian:

$$\begin{aligned} \hat{H} = & -2J_1[\hat{S}_1\hat{S}_3 + \hat{S}_4\hat{S}_6] - 2J_2[\hat{S}_1\hat{S}_2 \\ & + \hat{S}_4\hat{S}_5] - 2J_3[\hat{S}_2\hat{S}_3 + \hat{S}_5\hat{S}_6] - 2J_4[\hat{S}_3\hat{S}_4 \\ & + \hat{S}_1\hat{S}_6] - 2J_5\hat{S}_3\hat{S}_6 \end{aligned} \quad (1)$$

where \hat{S}_i are the local spin operators of each paramagnetic center. The calculated J values reproduce the experimental magnetic susceptibility curves (see Figure 4) reasonably well, taking into account the very large sensitivity of the shape of the curve with the J values.²⁰ From the calculated J values, we can extract some conclusions: (i) The total spin of the molecule is controlled by the nature of the exchange interactions (J_1 – J_3) in the Mn_3

(23) Stamatatos, T. C.; Foguet-Albiol, D.; Lee, S. C.; Stoumpos, C. C.; Raptopoulou, C. P.; Terzis, A.; Wernsdorfer, W.; Hill, S. O.; Perlepes, S. P.; Christou, G. *J. Am. Chem. Soc.* **2007**, *129*, 9484.

(24) Cano, J.; Cauchy, T.; Ruiz, E.; Milios, C. J.; Stoumpos, C. C.; Stamatatos, T. C.; Perlepes, S. P.; Christou, G.; Brechin, E. K. *Dalton Trans.* **2008**, 234.

(25) Ruiz, E.; Cirera, J.; Cano, J.; Alvarez, S.; Loose, C.; Kortus, J. *Chem. Commun.* **2008**, 5254.

(26) Piligkos, S.; Bendix, J.; Weihe, H.; Milios, C. J.; Brechin, E. K. *Dalton Trans.* **2008**, 2277.

(27) Rajaraman, G.; Murugesu, M.; Sañudo, C. E.; Soler, M.; Wernsdorfer, W.; Helliwell, M.; Chris, R. J.; Teat, S. J.; Christou, G.; Brechin, E. K. *J. Am. Chem. Soc.* **2004**, *126*, 15445.

(28) Ruiz, E.; Alvarez, S.; Cano, J.; Polo, V. *J. Chem. Phys.* **2005**, *123*, 164110.

(29) Ruiz, E.; Rodríguez-Fortea, A.; Tercero, J.; Cauchy, T.; Massobrio, C. *J. Chem. Phys.* **2005**, *123*, 074102.

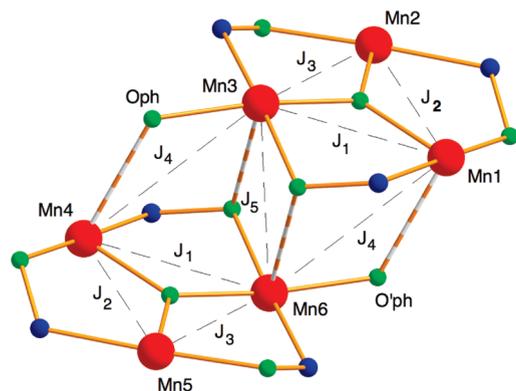


Figure 3. Description of the J values employed in the theoretical calculations.

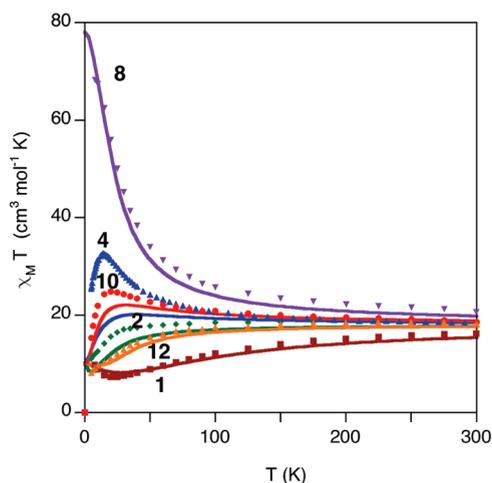


Figure 4. Representation of the magnetic susceptibility curves corresponding to the six studied Mn_6 complexes (see Table 2). The solid lines correspond to the curve obtained from the calculated J values while the marks are the experimental data.⁸

triangles through double oxo-oximate bridging ligands. (ii) The calculated values indicate that the J_1 interaction (see Figure 3), that corresponding to the edge of the Mn_3 triangle closest to its neighboring triangle, is ferromagnetic when it is associated with large $Mn-N-O-Mn$ torsion angles formed to complete the distorted octahedral coordination of the Mn^{III} cations of the neighboring Mn_3 triangle (see Figure 3). These long axial $Mn \cdots O$ bond distances represent the Jahn–Teller axes and through such interactions the two Mn_3 triangles are coordinated. However, for complexes **1** and **10** the $Mn-N-O-Mn$ torsion angle is small and the coupling is antiferromagnetic. Complex **1** should be carefully considered because it is the unique complex where there are axial carboxylato bridging ligands that produce a relatively large antiferromagnetic J_1 interaction; see similar cases with Mn_3 complexes in ref 24. Thus, there are three bridging ligands between the $Mn1-Mn3$ cations (see Figure 1), and the structure shows very small $Mn-N-O-Mn$ torsion angles in comparison with the other complexes because of the absence of large substituents in the *sao* ligand (see Table 2). (iii) The calculated J_2 and J_3 values, corresponding to oxo-oximate bridging ligands, show a nice correlation with the $Mn-N-O-Mn$ torsion angle (see Figure 5). Thus, large $Mn-N-O-Mn$ torsion

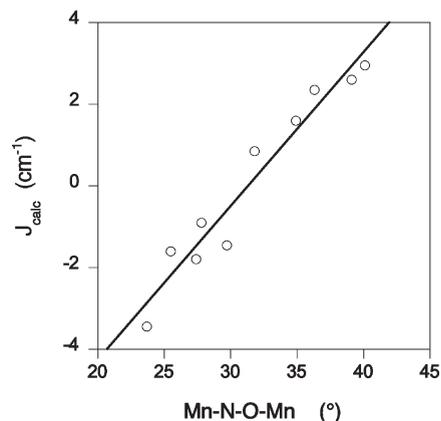


Figure 5. Representation of the dependence of the calculated J_2-J_3 values for the six studied complexes with the exception of complex **1** with the corresponding $Mn-N-O-Mn$ torsion angle for each interaction.

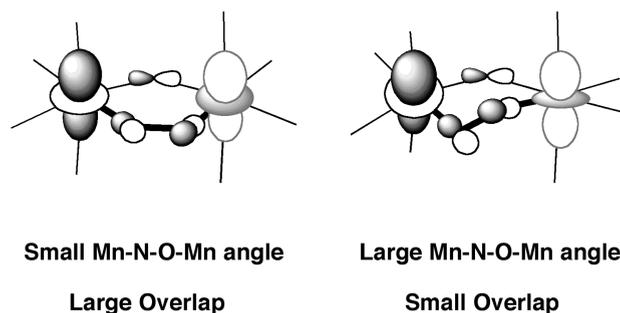


Figure 6. Plot to represent the change in the overlap between the d_{z^2} magnetic orbitals because of the distortion of the $Mn-N-O-Mn$ torsion angle.

angles result in a smaller overlap between the d_{z^2} magnetic orbitals giving ferromagnetic interactions (see Figure 6), as was previously assumed. (iv) The interactions between the triangles (J_4, J_5) are very similar for all complexes. The J_4 coupling through double oxo-oximate bridging ligands with two long $Mn \cdots O_{ph}$ bond distances gives a very weak antiferromagnetic interaction in most cases but is slightly ferromagnetic for complexes **8** and **12**, with the largest $Mn \cdots O_{ph}-Mn$ bond angles and relatively long $Mn-O_{ph}$ bond distances (see Supporting Information, Table S1). However, the J_5 interaction, corresponding to the two oxygen bridging ligands of the oximate groups is always ferromagnetic, and the calculated values are very similar for all complexes giving a predominant ferromagnetic character for the interaction between the two Mn_3 triangles. (v) The out-of-plane shifts of the central oxygen atom are relatively similar for all complexes with the exception of complex **1**; thus, it is not possible at this stage to establish its influence on the J values, but it must be analyzed in the next section. It is also worth noting that in all cases there is a very small energy difference between the first excited and the ground state, as pointed out by Carretta et al., indicating that a giant-spin model cannot be applied for the nesting of the different S manifolds.³⁰ An alternative representation using a model taking the Mn_3 moieties as the units for the giant-spin approximation

(30) Carretta, S.; Guidi, T.; Santini, P.; Amoretti, G.; Pieper, O.; Lake, B.; van Slageren, J.; El Hallak, F.; Wernsdorfer, W.; Mutka, H.; Russina, M.; Milios, C. J.; Brechin, E. K. *Phys. Rev. Lett.* **2008**, *100*, 157203.

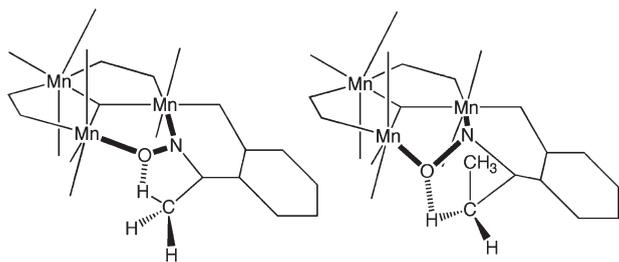


Figure 7. Description of distortion of the NO bridging ligand to form the intramolecular hydrogen bond for the *Me-sao* ligands (left) and *Et-sao* ligands (right). (see Supporting Information, Figure S1 for the pictures corresponding to the X-ray structure of this intramolecular contact for the whole family of complexes).

has been employed by Bahr et al. to study some tunneling transitions which are forbidden using such approximations for the whole Mn_6 complex.³¹

An important point to understand in the magnetism of the Mn_6 family is why the $Mn-N-O-Mn$ torsion angles are large or small. The analysis of the crystal structures reveals the existence of two factors controlling the magnetic behavior: the existence of an intramolecular hydrogen bond between the NO bridging ligand and the R substituent of the *sao* ligand (see Figure 7) and the presence of bulky substituents in terminal axial carboxylato ligands.⁸ The first factor has influence on the $Mn-N-O-Mn$ torsion angle for the J_2 and J_3 interactions while the substituents of the axial carboxylato ligands play an important role for the J_3 interactions; with the exception of complex **2** that has the carboxylato ligand coordinated to Mn2 instead of Mn3 (see Figure 3 and Supporting Information, Table S2) interacting with the equatorial *sao* ligand corresponding to the J_2 and J_3 interactions.

The analysis of the existence of an intramolecular hydrogen bond between the NO bridging ligand and the R substituent of the *sao* ligand, considering the presence of methyl or ethyl substituents, indicates that there are four different cases (see Supporting Information, for the representations of all these intramolecular interactions). (i) With the methyl substituent or without any substituent (*H-sao* ligand) there are no steric problems when forming the intramolecular $O \cdots H-C$ hydrogen bond (see Figure 7 left). Thus, the NO bridging ligands remain close to the Mn_3 plane, adopting relatively small $Mn-N-O-Mn$ torsion angles resulting in antiferromagnetic J_2 or J_3 interactions and the total spin is $S = 4$ (complexes **1**, **2**, **10**, and **16**). (ii) When the methyl substituent is present, there is a very long distance between the Mn_3 triangles and the $Mn-O$ distances are quite unusual inducing a distortion in the bridging ligand resulting in a larger $Mn-N-O-Mn$ torsion angle than expected giving large total spin values (complex **6**). (iii) When the ethyl substituent is present, the formation of the intramolecular hydrogen bond with the CH_2 moiety is hindered by the presence of the CH_3 group, resulting in a large $Mn-N-O-Mn$ torsion angle (see Figure 7, right), the ferromagnetic interactions are predominant because of the presence of large torsion angles and consequently, the total spin S is

12 (complexes **7–9**, **11**, **13**, and **15**). The experimental and theoretical results indicated a “magic angle” value, thus, if all the $Mn-N-O-Mn$ torsion angles are larger than 30 degrees, there is a predominance of the ferromagnetic interactions resulting in a $S = 12$ total spin value. (iv) When the ethyl substituent is present and there is no intramolecular hydrogen bond for some bridging ligands, the $Mn-N-O-Mn$ torsion angle is small (antiferromagnetic coupling) and the total spin is low (complexes **3–4**). In complex **12** there is an intermolecular hydrogen bond with a methanol molecule, not with a bridging ligand, resulting in the same effect as in the case of the lack of intramolecular interaction (torsion angle of 27.8°). Thus, the presence of solvent molecules in the crystal that can make hydrogen bond interactions with the bridging NO ligands would favor low spin states.

The presence of bulky substituents in the axial carboxylato ligands also affects the $Mn-N-O-Mn$ torsion angles, and consequently the magnetic properties. There are different coordinations of the carboxylato groups in the Mn_3 triangles (see Supporting Information, Table S2). Only in the case of complex **2** is the carboxylato group coordinated to the Mn2 (see Figure 3) while in all the other complexes it is always coordinated to Mn3. The effect of such carboxylato coordination is clearly reflected in the fact that in complex **2** the $Mn-N-O-Mn$ torsion angle corresponding to the J_2 and J_3 interactions are below 30° , in agreement with the two negative values calculated for such interactions. Thus, the presence of a bulky substituent in the carboxylato group induces smaller $Mn-N-O-Mn$ torsion angles in the two neighboring exchange pathways (usually J_1 and J_3 , see Figure 3). This fact is due to the steric repulsion of the carboxylato ligand with the aromatic ring of the *sao* ligand, resulting in a “flatter” equatorial coordination. This assumption can be clearly verified by the nice correlation found between the $Mn-N-O-Mn$ torsion angle and the angle between the plane containing the three manganese atoms and the plane of the six carbon atoms of the aromatic ring of the *sao* ligand (see Figure 8). The Mn_3-C_6 angle between these two planes measures the proximity of the ring with the R substituent of the carboxylato ligand, and consequently is related to the repulsion between them. It is worth pointing out that the $Mn-N-O-Mn$ torsion angles corresponding to the J_3 interactions are smaller with the exception of complexes **4** and **13** than those of the J_2 interaction, because there are the simultaneous effects of the intramolecular hydrogen bond and the presence of the bulky substituent. In conclusion, we can indicate that the size of the carboxylato ligand is important to mainly modify the J_3 exchange constant, thus, big substituents increase the repulsion with the equatorial ligands resulting in a smaller $Mn-N-O-Mn$ torsion angle and consequently, a large antiferromagnetic contribution.

We can therefore conclude that to have complexes with only ferromagnetic (or predominantly ferromagnetic) interactions to reach a total spin of $S = 12$, we need ethyl substituents (or even larger) in the R-*sao* ligand that will form a hindered intramolecular hydrogen bond introducing a distortion in the NO bridging ligand. The presence of external solvent molecules should be avoided, since these allow the formation of intermolecular hydrogen

(31) Bahr, S.; Milios, C. J.; Jones, L. F.; Brechin, E. K.; Mosser, V.; Wernsdorfer, W. *Phys. Rev. B* **2008**, *78*, 132401.

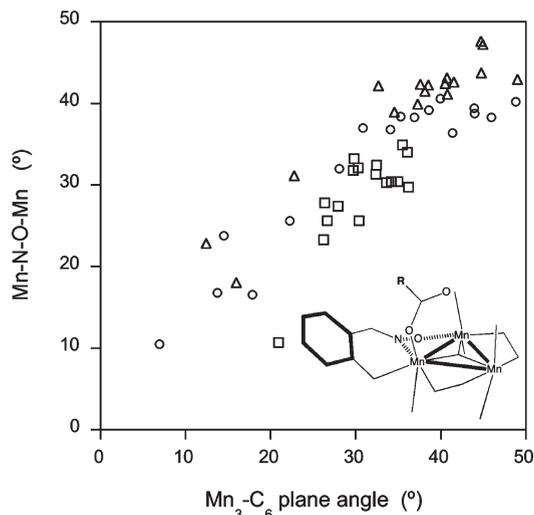


Figure 8. Dependence for the 16 Mn_6 complexes of the Mn–N–O–Mn torsion angles corresponding to the J_1 (triangles), J_2 (circles), and J_3 (squares) interactions with the angle between plane containing the three manganese atoms and that corresponding to the six carbon atoms of the aromatic ring of the *sao* ligand to show the influence of the steric effects due to the R substituent of the carboxylate ligand.

bonds that do not distort the bridging ligand. However, it is important to keep in mind that there is a subtle interplay at work here, because if the steric hindrance is too large, there is no intermolecular hydrogen bond. Also, the presence of bulky substituents in the axial carboxylato groups help to decrease the Mn–N–O–Mn torsion angle corresponding to the J_3 interaction. Thus, the choice of this substituent is also critical because of the repulsion with the phenyl ring of the *sao* ligand since too flat an equatorial coordination would result in a small Mn–N–O–Mn torsion angle and an antiferromagnetic interaction.

Magnetostructural Correlations. In this section, we want to check if the magnetism of the Mn_6 complexes is controlled solely by the Mn–N–O–Mn torsion angle or whether other structural parameters can simultaneously play an important role. From the analysis of the structures for the whole family of Mn_6 complexes, there are three structural parameters that show relatively important changes between the different complexes: (i) the Mn–N–O–Mn torsion angles, (ii) the out-of-plane shifts of the oxo bridge in the center of the Mn_3 triangles, and (iii) the length of the long $Mn \cdots O_{ph}$ axial bond distances (because of the Jahn–Teller effects) that control the distance between the two Mn_3 triangles. We will focus our study on the two first parameters because they directly affect the interactions that control the total spin of the molecule. We have employed the structure of complex **2** (see Figure 9) as a reference to study the influence of these two structural parameters. This complex shows relatively small Mn–N–O–Mn torsion angles because of the presence of the carboxylato group coordinated to the Mn2 atom, and consequently the J_2 and J_3 interactions are antiferromagnetic.

To check the influence of the Mn–N–O–Mn torsion angle, we have introduced modifications in the two torsion angles corresponding to the J_2 and J_3 interactions. To independently analyze the effects in these two exchange constants, we have modified only one of the angles for each model structure, keeping the rest of the

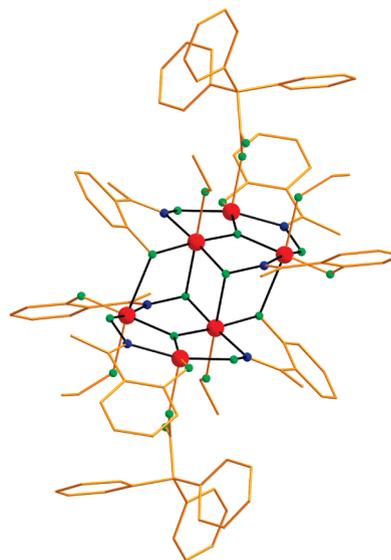


Figure 9. Representation of the molecular structure of complex **2**. Large red spheres are the Mn atoms, while oxygen and nitrogen atoms are represented by small green and blue spheres, respectively. The carbon atoms are represented as orange cylinders to simplify the figure.

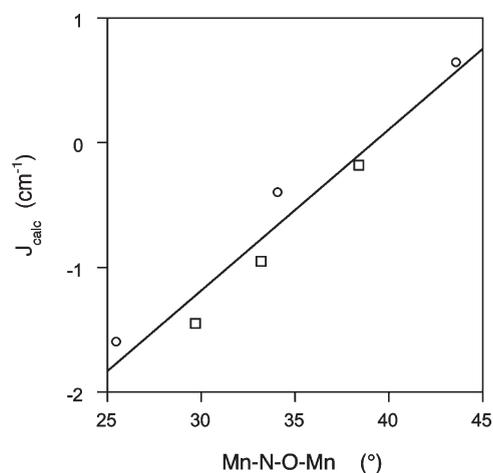


Figure 10. Dependence of the calculated J_2 (circles) and J_3 (squares) exchange coupling constants with the Mn–N–O–Mn torsion angle for the modified **2** complex.

structure “frozen” as well as the Mn–O and Mn–N bond distances of the modified bridging ligand. The other exchange interactions remain essentially constant, and the dependence of the J values with the distortions is represented in Figure 10. As expected from the correlation found for the calculated J values for the set of whole structures (Figure 5), the increase in the value of the Mn–N–O–Mn torsion angle reduces the antiferromagnetic contribution resulting in ferromagnetic behavior for large torsion angle values, in agreement with the change in the overlap between the magnetic orbitals represented in Figure 6. The analysis of the total energies indicates that for instance the energy difference between the original complex (**2**) and the most distorted complex corresponding to the J_3 interaction (change in Mn–N–O–Mn angle from 29.7 to 38.4°) is only 2 kcal/mol. The small difference energy indicates that the Mn–N–O–Mn angle is relatively flexible, and the gain in energy obtained

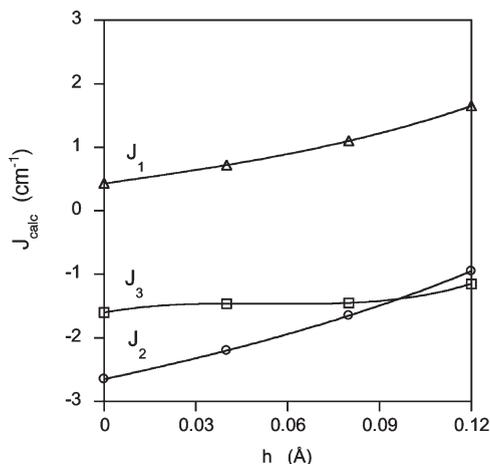


Figure 11. Dependence of the calculated J_1 (triangles), J_2 (circles), and J_3 (squares) exchange coupling constants with the out-of-plane shift of the central oxo bridging ligand for the modified **2** complex.

to improve the intramolecular hydrogen bond interaction or the steric repulsion caused by the bulky substituents of the axial carboxylato groups can modify the Mn–N–O–Mn torsion angle. However, it is worth noting that for the largest Mn–N–O–Mn angles the calculated values using the distorted complex are slightly less ferromagnetic than those obtained for the whole structures (see Table 2). Hence, it seems reasonable to suggest that there are other structural parameters that play a significant role in the exchange interaction within the Mn₃ triangles.

The influence of the out-of-plane shift of the central oxo bridging ligands was pointed out in previous papers as a possible important magnetostructural parameter. However, at first glance only complex **1** shows a relatively large shift of 0.228 Å. The calculated J values using complex **2** are represented in Figure 11. The three exchange interactions corresponding to the Mn₃ triangles (J_1 – J_3) show a decrease in the antiferromagnetic contribution to the J values when the out-of-plane shift is larger, consistent with the simple idea that the overlap between the magnetic orbitals should be smaller. However one never sees a switch in the exchange from antiferromagnetic to ferromagnetic. This is also consistent with more recent studies on [Mn₃-oximate] complexes that seem to show little correlation between the out-of-plane shift and the sign of the exchange.³² The smaller variation of the J_3 exchange coupling constant occurs because the changes on the Mn–O distances involved in the J_3 interaction are smaller because the employed model is a real structure and not a symmetric model.

Spin Densities. The distribution of the spin densities on the Mn₆ complexes shows a considerable localization on the Mn^{III} centers. The Mulliken population values for these cations are always around 3.8–3.9 e⁻, very close to the formal value of 4 expected for a Mn^{III} cation. Previously, we have seen a small tendency for paramagnetic centers with many unpaired electrons to delocalize them on to the ligands.³³ The Mn^{III} cations show a quasi-spherical spin density (see Figure 12) with some hollows correspond-

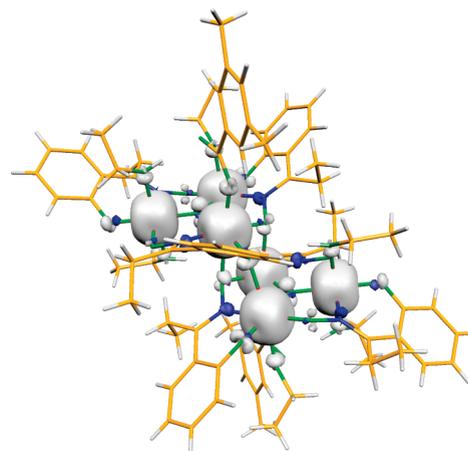


Figure 12. Representation of the spin density corresponding to the ferromagnetically coupled $S = 12$ ground state of complex **8**. The isodensity surface represented corresponds to a value of 0.01 e⁻/bohr³ (white and blue regions indicate positive and negative spin populations, respectively).

ing to the empty $d_{x^2-y^2}$ orbital.³⁴ Consequently, spin delocalization on to the oxygen atoms of the axial ligands is larger than for the equatorial ones (despite the longer Mn–X bond distances), and this has been previously witnessed in a Mn^{III} oxo centered triangle.³⁵ The delocalization on the oxygen atoms corresponding to the anionic carboxylate ligands is slightly more important than on the neutral ethanol molecules. For the equatorial oxygen atoms there are two different regions, a positive spin density with π character due to the delocalization of the half-occupied t_{2g} orbitals, and a σ region of small negative spin density due to the absence of unpaired electrons in the manganese $d_{x^2-y^2}$ orbitals. The spin densities in the bridging nitrogen atoms are negative indicating a spin polarization mechanism and the lack of π delocalization showing a different behavior between the two atoms in the bridging ligand.

Concluding Remarks

Theoretical methods based on DFT allow calculation of the exchange coupling constants in complex polynuclear systems, such as those of the family of Mn₆ complexes studied in this paper. Thus, it is possible to obtain a set of exchange coupling constants that reproduces the experimental magnetic susceptibility curves using theory, where it is almost impossible to extract a proper set of fitted (experimental) values because of overparametrization problems. The calculated exchange coupling constants in the Mn₃ triangle subunits show a correlation with the Mn–N–O–Mn torsion angles, larger angles provide ferromagnetic couplings leading to high spin complexes ($S = 12$). These torsion angles are controlled by the presence of intramolecular hydrogen bond interactions in the case of the J_2 interactions, while for J_3 the presence of bulky substituents in the carboxylato ligands also play an important role. Relatively large substituents in the *sao* ligands, such as ethyl groups, induce a large distortion of the oximate bridging ligand to make a hindered

(32) Inglis, R.; Jones, L. F.; Mason, K.; Perlepes, S. P.; Wernsdorfer, W.; Brechin, E. K. *Chem.—Eur. J.* **2008**, *14*, 9117.

(33) Cano, J.; Ruiz, E.; Alvarez, S.; Verdaguier, M. *Comments Inorg. Chem.* **1998**, *20*, 27.

(34) Ruiz, E.; Cirera, J.; Alvarez, S. *Coord. Chem. Rev.* **2005**, *249*, 2649.

(35) Jones, L. F.; Rajaraman, G.; Brockman, J.; Murugesu, M.; Sañudo, E. C.; Raftery, J.; Teat, S. J.; Wernsdorfer, W.; Christou, G.; Brechin, E. K.; Collison, D. *Chem.—Eur. J.* **2004**, *10*, 5180.

intramolecular hydrogen bond. Hence, small substituents, for instance methyl groups or non-substituted ligands, give undistorted bridging ligands favoring antiferromagnetic couplings and consequently, low spin states ($S = 4$). The substituents of the axial carboxylato ligands play an important role in the Mn–N–O–Mn torsion angles, especially so for the J_3 exchange constant, large substituents providing a repulsion with the phenyl ring of the equatorial *sao* ligand flattening the Mn–N–O–Mn torsion angle.

The out-of-plane shift of the central oxo bridging ligands of the Mn_3 subunits plays a less important role in the exchange interactions than the Mn–N–O–Mn torsion angles, but larger shifts do appear to reduce the antiferromagnetic contributions. The influence of both structural parameters can be easily understood as the loss of overlap between the magnetic orbitals.

The spin density analyzed for a high spin complex with ground state $S = 12$ shows a large localization on the Mn^{III} cations. The empty $d_{x^2-y^2}$ orbitals of such cations make spin polarization the predominant mechanism on the equatorial nitrogen atoms, while the oxygen equatorial atoms show an important π delocalization contribution because of mixture with the t_{2g} orbitals of the cations bearing unpaired electrons. The coordinated oxygen atoms of the axial ligands show positive spin density values because of the delocalization of the spin density corresponding to the d_{z^2} orbitals.

Computational Details

In our calculations, we employed the experimental structures that take into account small structural effects induced by intermolecular interactions that may result in significant changes in the calculated exchange coupling constants, because of the strong dependence of the magnetic properties on structural parameters. All the calculations with the B3LYP functional³⁶ were performed with the Gaussian03 code,³⁷ in some cases we employed the NWChem code^{38,39} to verify some results, using the quadratic convergence

approach and a guess function generated with the Jaguar 6.5 code.⁴⁰ The triple- ζ all electron Gaussian basis set proposed by Schaefer et al. was employed for all the atoms.⁴¹

To obtain the five exchange coupling constants for each Mn_6 complex we used a least-squares fitting using the energies corresponding to nine spin configurations: a high spin solution ($S = 12$), three $S = 8$ distributions with the inversion of only one spin {Mn1}, {Mn2}, and {Mn3}, three $S = 4$ configurations with negative spin at two Mn^{III} cations {Mn2, Mn5}, {Mn1, Mn4}, and {Mn3, Mn6}, and finally two $S = 0$ configurations with negative spin at three Mn^{III} cations {Mn1, Mn2, Mn3} and {Mn1, Mn4, Mn5}. In the fitting procedure to obtain the five J values for each Mn_6 complex, the standard deviations are lower than 0.1 cm^{-1} with the exception of complex **4** (see Supporting Information, Table S3). The calculation of the J values were done using the non spin-projected approach^{22,28} because the spin projected method^{42,43} or that proposed by Yamaguchi and co-workers⁴⁴ results in an overestimation of the J values because of the presence of self-interaction error (SIE) in the usual functionals, such as B3LYP. The SIE mimics some static correlation contributions and this fact provides an overstabilization of the low spin states that it is avoided in the non-projected approach.

Acknowledgment. The research reported here was supported by the *Ministerio de Ciencia e Innovación* and *Generalitat de Catalunya* through Grants CTQ2008-06670-C02-01 and 2005SGR-00036, respectively. The authors thankfully acknowledge the computer resources, technical expertise, and assistance provided by the Barcelona Supercomputing Center (*Centro Nacional de Supercomputación*). E.K.B. would like to thank the Leverhulme Trust for funding.

Supporting Information Available: Table S1 and S2 with the structural parameters for the J_4 and J_5 interactions and the coordination of the axial terminal ligands, respectively. References 37 and 38 in full. Cartesian coordinates and calculated energies of the studied Mn_6 complexes. This material is available free of charge via the Internet at <http://pubs.acs.org>.

(36) Becke, A. D. *J. Chem. Phys.* **1993**, *98*.

(37) Frisch, M. J. et al. *Gaussian 03*, Revision C.1; Gaussian, Inc: Pittsburgh, PA, 2003.

(38) Aprà, E. et al. *NWChem 4.7*; Richland, WA, 99352-0999, 2005.

(39) Kendall, R. A.; Apra, E.; Bernholdt, D. E.; Bylaska, E. J.; Dupuis, M.; Fann, G. I.; Harrison, R. J.; Ju, J. L.; Nichols, J. A.; Nieplocha, J.; Straatsma, T. P.; Windus, T. L.; Wong, A. T. *Comput. Phys. Commun.* **2000**, *128*, 260.

(40) *Jaguar 6.5*; Schrödinger, Inc.: Portland, 2005.

(41) Schaefer, A.; Huber, C.; Ahlrichs, R. *J. Chem. Phys.* **1994**, *100*, 5829.

(42) Noodleman, L. *J. Chem. Phys.* **1981**, *74*, 5737.

(43) Caballol, R.; Castell, O.; Illas, F.; Moreira, I. de P. R.; Malrieu, J.-P. *J. Phys. Chem. A* **1997**, *101*, 7860.

(44) Nishino, M.; Yoshioka, Y.; Yamaguchi, K. *Chem. Phys. Lett.* **1998**, *297*, 51.